bioRxiv preprint doi: https://doi.org/10.1101/633099; this version posted May 14, 2019. The copyright holder for this preprint (which was not certified by peer review) is the author/funder. All rights reserved. No reuse allowed without permission.

Various components of the RNAi pathway are required for conidiation, ascosporogenesis, virulence, DON production and SIGS-mediated fungal inhibition by exogenous dsRNA in the Head Blight pathogen *Fusarium graminearum*

Fatima Yousif Gaffar[1†], Jafargholi Imani[1†], Petr Karlovsky[2], Aline Koch[1], Karl-Heinz Kogel[1]

[1] Department of Phytopathology, Centre for BioSystems, Land Use and Nutrition, Justus Liebig University, Heinrich-Buff-Ring 26-32, D-35392, Giessen, Germany

[2] Department of Crop Sciences, Molecular Phytopathology and Mycotoxin Research, University of Goettingen, D-37077 Goettingen, Germany

Email addresses:

Fatima.Y.Gaffar@agrar.uni-giessen.de

Jafargholi.Imani@agrar.uni-giessen.de

pkarlov@gwdg.de

Aine.Koch@agrar.uni-giessen.de

Karl-Heinz.Kogel@agrar.uni-giessen.de

*Correspondence to Karl-Heinz.Kogel@agrar.uni-giessen.de

[†] Contributed equally to this work.

bioRxiv preprint doi: https://doi.org/10.1101/633099; this version posted May 14, 2019. The copyright holder for this preprint (which was not certified by peer review) is the author/funder. All rights reserved. No reuse allowed without permission.

Abstract:

Gene silencing through RNA interference (RNAi) shapes many biological processes in filamentous fungi. In this study we explored the contribution of several key proteins of fungal RNAi pathways, including DICER-like1 and 2 (FgDCL1, FgDCL2), ARGONAUTE1 and 2 (FgAGO1, FgAGO2), AGO-interacting protein FgQIP (QDE2-interacting protein), RecQ helicase (FgQDE3), and four RNA-dependent RNA polymerases (FgRdRP1, FgRdRP2, FgRdRP3, FgRdRP4), to sexual and asexual multiplication, pathogenicity as well as spray-induced gene silencing (SIGS) by exogenous dsRNA of the ascomycete fungus *Fusarium graminearum* (*Fg*). We corroborate and extend earlier findings that conidiation, ascosporogenesis and Fusarium Head Blight (FHB) symptom development require operable RNAi pathways. Of note, the involvement of RNAi components in conidiation is dependent on environmental conditions as it is detectable only under low light (< 2 µmol m^{-2} s^{-1}). Although both DCLs and AGOs partially share their functions, the sex-specific RNAi pathway (ascosporogenesis) is mediated primarily by FgDCL1 and FgAGO2, while the RNAi components FgDCL2 and FgAGO1 contribute to conidia formation and germination. Similarly, FgDCL1 and FgAGO2 account for pathogenesis as their knock-out (KO) results in reduced FHB development. Apart from *Δdcl2* and *Δago1*, the KO mutants *Δrdrp2*, *Δrdrp3*, *Δrdrp4*, *Δqde3* and *Δqip* are strongly compromised for conidiation, while KO mutations in all RdPRs, QDE3 and QIP strongly affect ascosporogenesis. Analysis of trichothecenes mycotoxins in wheat kernels showed that the relative amount of DON [rDON], calculated as [DON] per amount of fungal genomic DNA, was reduced in all spikes infected with RNAi mutants, suggesting that fungal RNAi pathways affect *Fg*'s DON production in wheat spikes. Moreover, SIGS-mediated plant protection to Fusarium was strongly dependent on fungal DCLs, AGOs, and QIP, but not on QDE3. Together these data show that in *F. graminearum* the RNAi machinery plays a central role in different steps of sexual and asexual reproduction, in fungal pathogenicity and DON production, and in the control of the pathogen by exogenous dsRNA under the tested conditions.

bioRxiv preprint doi: https://doi.org/10.1101/633099; this version posted May 14, 2019. The copyright holder for this preprint (which was not certified by peer review) is the author/funder. All rights reserved. No reuse allowed without permission.

Introduction:

RNA interference (RNAi) is a conserved mechanism triggered by double-stranded (ds)RNA that mediates resistance to exogenous pathogenic nucleic acids, regulates the expression of protein-coding genes on the transcriptional and posttranscriptional level and preserves gene stability by transposon silencing (Fire et al., 1998; Mello et al., 2004; Hammond, 2005; Baulcombe 2013). Many reports have demonstrated that this natural mechanism for sequence-specific gene silencing also holds promise for experimental biology and offers practical applications in functional genomics, therapeutic intervention, and agriculture (Nowara et al., 2010; Koch and Kogel, 2014; Cai et al., 2018; Zanini et al., 2018). The core RNAi pathway components are conserved in eukaryotes, including nearly all parasitic and beneficial fungi (Cogoni and Macino, 1999; Dang et al., 2011; Carreras-Villaseñor et al., 2013; Torres-Martínez and Ruiz-Vázquez, 2017): DICER-like (DCL) enzymes, which belong to the RNase III superfamily, initiate the RNAi pathway by generating small interfering (si)RNA and micro (mi)RNAs (Meng et al., 2017; Song and Rossi, 2017); ARGONAUTE (AGO) superfamily proteins bind small RNAs (sRNAs) to form an RNA-induced silencing complex (RISC) for transcriptional and post-transcriptional gene silencing (Zhang et al., 2015; Nguyen et al., 2018) and RNA-dependent RNA polymerases (RdRPs) are involved in the production of dsRNA that initiate the silencing mechanism as well as in the amplification of the silencing signal through secondary RNA (Calo et al., 2012).

Fungal RNAi pathways contribute to genome protection (Meng et al. 2017), pathogenicity (Weiberg et al., 2013; Kusch et al., 2018, development (Carreras-Villaseñor et al., 2013), and antiviral defense (Segers et al., 2007; Campo et al., 2016. In *Aspergillus flavus* (Bai et al., 2015), *Magnaporthe oryzae* (Raman et al., 2017) and *Penicillium marneffei* (Lau et al., 2013), sRNAs were shown to be responsive to environmental stress. In *Trichoderma atroviride*, both light-dependent asexual reproduction and light-independent hyphal growth require an operational RNAi machinery (Carreras-Villaseñor et al., 2013). Similarly, in *Mucor circinelloides,* defects in the RNAi machinery resulted in various developmental defects such as dysfunction during sexual and asexual reproduction (Torres-Martínez and Ruiz-Vázquez, 2017).

Neurospora crassa, a model organism for studying gene silencing pathways in filamentous fungi, has two different silencing pathways, namely quelling (Romano et al., 1992) and meiotic silencing by unpaired DNA (MSUD) (Shiu et al., 2001). In the vegetative stage, the introduction of repetitive DNA sequences triggers posttranscriptional gene silencing of all homologous genes, an RNAi silencing phenomenon known as quelling, while MSUD is associated with the sexual cycle. *QDE3* (*Quelling defective3*), which encodes a RecQ helicase, and RPA (subunit

bioRxiv preprint doi: https://doi.org/10.1101/633099; this version posted May 14, 2019. The copyright holder for this preprint (which was not certified by peer review) is the author/funder. All rights reserved. No reuse allowed without permission.

of replication protein A) which recognizes aberrant DNA structures and recruits QDE1 (Quelling defective1), which is a RdRP, to the ssDNA locus, resulting in production of aberrant RNAs and its conversion to dsRNAs. Subsequently the dsRNA is processed into sRNA duplexes by DCL1. The sRNAs are loaded onto QDE2 (Quelling defective2), which encodes an AGO homolog. QDE2 cleaves the passenger strand and the putative exonuclease QIP (QDE2-interacting protein) removes it to form an active RISC that targets complementary mRNA for degradation (Chang et al., 2012).

MSUD, on the other hand, occurs during sexual development in prophase I of meiosis, when unpaired homologous DNA sequences have been detected during the pairing of the homologous chromosomes, which leads to the production of aberrant RNA transcripts (Chang et al., 2012). Components of the RNAi machinery involved in MSUD are also important for ascospore formation in *N. crassa* (Shiu et al., 2001; Alexander et al., 2008; Lee et al., 2003).

Fusarium graminearum (*Fg*) is one of the most devastating pathogens of many cereals causing Fusarium Head Blight (FHB) and Crown Rot (FCR). The pathogen belongs to the filamentous ascomycetes (Dean et al., 2012; Urban et al., 2015; Brown et al., 2017). The fungus reproduces using sexual spores (ascospores) and asexual conidia. Ascospores are the primary inoculum for FHB epidemics, because these spores are forcibly shot into the environment and can pass long distances (Maldonado-Ramirez et al., 2005). Moreover, the sexual development warrants the formation of survival structures necessary for overwintering (Dill-Macky and Jones, 2000) and the genetic diversity of the population (Cuomo et al. 2007). Importantly, fungi of the genus Fusarium contaminate the grain with mycotoxins and thus decrease grain quality Harris et al., 2016). Among the mycotoxins, the B group trichothecenes, including deoxynivalenol (DON), nivalenol (NIV), and their acetylated derivatives (3A-DON, 15A-DON, and 4A-NIV) influence the virulence of the fungus (Ilgen et al., 2009; Desjardins et al., 1993; Jansen et al., 2005). It has been suggested that mycotoxins such as DON trigger an oxidative burst in the host plants, resulting in cell necrosis and disintegration of the defense system, which then favors colonization of the plant tissues by a necrotrophic fungus (Audenaert et al., 2014).

To develop RNAi-based plant protection strategies such as host-induced gene silencing (HIGS) (Koch et al. 2013) and spray-induced gene silencing (SIGS) (Koch et al., 2016; Koch et al. 2018) against Fusarium species, it is required to bank on knowledge about the RNAi components involved in Fusarium development and pathogenicity. Of note, a report of Chen and colleagues (Chen et al., 2015) demonstrated that, in *Fg*, a hairpin RNA (hpRNA) can efficiently silence the expression level of a target gene, and that the RNAi components FgDCL2 and FgAGO1 are required for silencing. This finding is partially consistent with

bioRxiv preprint doi: https://doi.org/10.1101/633099; this version posted May 14, 2019. The copyright holder for this preprint (which was not certified by peer review) is the author/funder. All rights reserved. No reuse allowed without permission.

reports showing that a *Fg* wild type (wt) strain, but not *Fg* RNAi mutants, are amenable to target gene silencing, when it grows on a plant sprayed with exogenous dsRNA directed against the fungal *Cytochrome P450 lanosterol C-14α-demethylase* (*CYP51*) gene (Koch et al., 2016).

F. graminearum possesses a functional MSUD mechanism (Son et al., 2011). The *AGO* genes *FgSMS2* or *FgAGO2* are necessary for sexual reproduction Kim et al., 2015). A more recent work discovered that the sex-induced RNAi mechanism had important roles in sexual reproduction of the fungus (Son et al., 2017). siRNAs produced from exonic gene regions (ex-siRNAs) participated in post-transcriptional gene regulation at a genome-wide level in the late stages of sexual reproduction (Son et al., 2017). The sex-specific RNAi pathway was primarily governed by FgDCL1 and FgAGO2. Thus, *F. graminearum* primarily utilizes ex-siRNA-mediated RNAi for ascospore formation. Consistent with the key role of FgDCL1 in generative development, the combination of sRNA and transcriptome sequencing predicted 143 novel microRNA-like RNAs (milRNAs) in wild-type perithecia, of which most were depended on FgDCL1. Given that 117 potential target genes were predicted, these perithecium-specific milRNAs may play roles in sexual development (Zeng et al., 2018).

In this study, we extended these previous studies to address the requirement of an extended set of *F. graminearum* RNAi genes in growth, reproduction, virulence, and toxin production.

bioRxiv preprint doi: https://doi.org/10.1101/633099; this version posted May 14, 2019. The copyright holder for this preprint (which was not certified by peer review) is the author/funder. All rights reserved. No reuse allowed without permission.

Results:

Core components of the RNAi pathway of *F. graminearum* are not required for light induced conidiation

The *Fg* genome obtained from the Broad Institute (www.broadinstitute.org) contains many functional RNAi machinery components (Chen et al., 2015; Son et al., 2017). We generated *Fg* gene replacement mutants for several major RNAi genes by homolog recombination using the pPK2 binary vector (Tab. 1). Disruption vectors for *FgDCL1*, *FgDCL2*, *FgAGO1*, *FgAGO2*, *FgRdRP1*, *FgRdRP2*, *FgRdRP3*, *FgRdRP4*, *FgQDE3*, and *FgQIP* were constructed by inserting two flanking fragments (~1000 bp) upstream and downstream of the corresponding genes in pPK2 vector (Table S1; Fig. S1). The vectors were introduced into *Agrobacterium tumefaciens*, followed by agro-transformation of the *Fg* strain IFA65. Transformants were transferred to Petri dishes of potato extract glucose (PEG) medium, containing 150 µg/ml hygromycin and 150 µg/ml ticarcillin. Respective mutants were verified by PCR analysis with genomic DNA as template (Fig. 1) and by expression analysis of the respective RNAi gene (Fig. S2). Colony morphology of PCR verified mutants (see methods, 12h/12h light/dark) was inspected in axenic cultures of three different media, PEG, synthetic nutrient (SN) agar and starch agar (SA). In the PEG agar medium, all mutants showed slightly reduced radial growth, while there were no clear differences as compared with the IFA65 (wt) strain in SN and SA media (Fig. S3 A-C). In liquid PEG medium under day light conditions, all mutants produced comparable amounts of mycelium biomass, though different amounts of the red pigment aurofusarin (Frandsen et al., 2006): *Δdcl1*, *Δdcl2*, *Δrdrp1*, *Δqde3,* and *Δqip1* showed reduced pigmentation, while *Δago1*, *Δrdrp2*, *Δrdrp3*, and *Δrdrp4* showed higher pigmentation compared to wt IFA65 (Fig. S3 D). Under light induction conditions (12 h light; 52 µmol m^{-2} s^{-1}), conidia grown in 96-well-plate liquid SN cultures showed normal germ tube emergence (not shown). All RNAi mutants formed an elongated hyphal cell type, producing abundant conidia on conidiophores and directly from hyphae. Conidia were moderately curved with clear septations.

In absence of light induction conidiation of *F. graminearum* is influenced by RNAi pathway genes

When grown continuously under dimmed light (2 µmol m^{-2} s^{-1}), liquid SN cultures of RNAi mutants showed significantly reduced conidiation compared to wt IFA65, except *Δago2* and *Δrdrp1*, which were only slightly affected (Fig. 2 A). Under this non-inductive condition, some RNAi mutants also were compromised in conidial germination: *Δago1*, *Δago2* and *Δrdrp4*

bioRxiv preprint doi: https://doi.org/10.1101/633099; this version posted May 14, 2019. The copyright holder for this preprint (which was not certified by peer review) is the author/funder. All rights reserved. No reuse allowed without permission.

showed significantly reduced germination, while *Δrdrp3*, *Δdcl1*, *Δrdrp1* and *Δdcl2* showed a slight reduction, and *rdrp2*, *Δqip* and *Δqde3* showed normal conidial germination (Fig. 2 B). All RNAi mutants had a normal germ tube morphology, except *Δrdrp4*, which tends to develop multiple germ tubes (Fig. 2 C). These results suggest a requirement for *Fg* RNAi components genes in the full control of asexual development depending on the environmental conditions.

F. graminearum RNAi components are required for sexual development

Because there were contrasting data in the literature, we resumed asking the question of whether RNAi components are requirement for sexual reproduction. Perithecia (fruiting bodies) formation was induced in carrot agar axenic cultures (Cavinder et al., 2012). All RNAi mutants produced melanized mature perithecia in nearly the same numbers compared to wt IFA65 (not shown). Next we assessed the forcible discharge of ascospores by a spore discharge assay (Fig. 3). Discharge of ascospores from perithecia into the environment results from turgor pressure within the asci; the dispersal of ascospores by forcible discharge is a proxy for fungal fitness as it is important for dissemination of the disease. To this end, half circular agar blocks covered with mature perithecia were placed on glass slides and images from forcibly fired ascospores (white cloudy) were taken after 48 h incubation in boxes under high humidity and fluorescent light. We found that the forcible discharge of ascospores was severely compromised in *Δdcl1*, *Δago2*, *Δrdrp1*, *Δrdrp2*, *Δqde3*, and less severe in *Δdcl2*, *Δago1*, *Δqip1*, while *Δrdrp3* and *Δrdrp4* were indistinguishable from the wt IFA65. (Fig. 3 A,B). Microscopic observation of the discharged ascospores revealed that their morphology was not affected (not shown). The percentage of discharged ascospores that retained the ability to germinate varied in the mutants with *Δrdrp3* and *Δrdrp4*, showing strong reduction in the ascospore germination (Fig. 3 C). Together these results support the notion that the RNAi pathway is involved in sexual reproduction. Consistent with Son et al. (2017), especially DCL1 and AGO2 have important roles in sexual reproduction in *Fusarium graminearum* by producing siRNAs (ex-siRNAs) from gene regions.

F. graminearum RNAi mutants show variation in kernel infection

It was reported that *Fg* mutants defective in DCL, AGO, or RdRP were not compromised in virulence on wheat spikes (Chen et al., 2015). We extended this previous study by testing additional *Fg* RNAi mutants. Conidia were point-inoculated to a single spikelet at the bottom of a spike of the susceptible wheat cultivar Apogee. Fungal colonization was quantified 9 and 13 days post inoculation (dpi) by determining the infection strength. Infected parts of a spike

bioRxiv preprint doi: https://doi.org/10.1101/633099; this version posted May 14, 2019. The copyright holder for this preprint (which was not certified by peer review) is the author/funder. All rights reserved. No reuse allowed without permission.

bleached out, whereas the non-inoculated spikes remained symptomless. We found that, at late infection stages (13 dpi), all RNAi mutants caused strong FHB symptoms on wheat spikes comparable with wt IFA65 (Fig. 4 A). However, there were clear differences in the severity of infections at earlier time points (9 dpi), with *Δdcl1* and *Δago2* showing a most compromised FHB development. At 13 dpi, RNAi mutants also showed considerable variation on *Fg*-infected kernel morphology (Fig. S4 A). Thousand-grain-weight (TGW) of kernels infected with RNAi mutants showed slight, though not significant differences, in the total weights compared to wt IFA65 infection (Fig. S4B).

DON production is compromised in *F. graminearum* mutants that show reduced pathogenicity on wheat kernel

We quantified the amount of the mycotoxin DON in *Fg*-infected wheat spikes at 13 dpi (point-inoculation using 5 µl of 0.002% Tween 20 water containing 40,000 conidia / mL) at mid-anthesis. Of note, the relative amount of DON [rDON], calculated as [DON] per amount of fungal genomic DNA, was reduced in virtually all spikes infected with RNAi mutants, whereby [rDON] was strongly reduced especially in spikes colonized with mutants *Δago1*, *Δrdrp1*, *Δrdrp2*, *Δrdrp3*, *Δrdrp4* and *Δqde3* as compared with wt IFA65 (Tab. 2). The data suggest that fungal RNAi pathways affect *Fg*'s DON production in wheat spikes. While [rDON] changed, the ratio of [DON] and [A-DON] (comprising 3A-DON and 15A-DON) remained constant in all mutants vs. IFA65, suggesting that the fungal RNAi pathways do not affect the trichothecene metabolism.

***F. graminearum* mutants *Δdcl1*, *Δdcl2*, *Δago1*, *Δago2*, *Δrdrp1* and *Δqip* are compromised in SIGS**

Next, we addressed the question which RNAi mutants are compromised in spray-induced gene silencing (SIGS). It has been shown that spraying leaves or fruits with dsRNA targeting essential fungal genes, results in substantial protection from infection and disease (Koch et al., 2016; Wang et al., 2016; Dalakouras et al., 2016; McLoughlin et al., 2018). Moreover, it was shown that a hairpin RNA (hpRNA) can efficiently silence the expression level of a fungal target gene, and that the RNAi components FgDCL2 and FgAGO1 are required for silencing (Chen et al., 2015). Similarly, a *Fgdcl1* mutant was compromised in SIGS, e.g. showing insensitivity to application of CYP3RNA, a dsRNA targeting the three fungal genes *FgCYP51A*, *FgCYP51B* and *FgCYP51C* (Koch et al., 2016). To extend these findings, we conducted a SIGS experiment on detached barley leaves that were sprayed with 20 ng μL^{-1} CYP3RNA. After 48 h leaves were drop inoculated with 5 x 10^4 conidia ml^{-1} of RNAi mutants.

bioRxiv preprint doi: https://doi.org/10.1101/633099; this version posted May 14, 2019. The copyright holder for this preprint (which was not certified by peer review) is the author/funder. All rights reserved. No reuse allowed without permission.

241 Upon five days, infected leaves were scored for disease symptoms and harvested afterwards to
242 measure the expression of the three fungal target genes by qPCR (Fig. 5). As revealed by
243 reduced disease symptoms in treatments of leaves with CYP3RNA vs. TE (buffer control), a
244 SIGS effects was retained in the IFA65 wt and the corresponding mutant *Δqde3*. All other
245 mutants tested in this experiment were slightly or strongly compromised in SIGS: In *Δago1*,
246 *Δago2*, *Δrdrp1* there was no difference in the infection strength between CPY3RNA-treated vs.
247 TE-treated mutants, while *Δdcl1*, *Δdcl2* and *Δqip1* showed even higher infection upon
248 CYP3RNA vs. TE treatment (Fig. 5 A). Consistent with this, strong down-regulation of all three
249 *CYP51* target genes was observed only in the IFA65 wt and *Δqde3*, while mutants *Δago1*, *Δago2*,
250 *Δrdrp1*, showed some down-regulation of single *CYP51* genes. Moreover, in *Δdcl1*, *Δdcl2* and
251 *Δqip1*, the inhibitory effect of CYP3RNA on *FgCYP51A*, *FgCYP51B* and *FgCYP51C*
252 expression was completely abolished (Fig. 5B). To further substantiate this finding, we tested
253 a *dcl1 dcl2* double mutant in *Fg* strain PH1. As anticipated from the experiments with the IFA65
254 strain, the PH1 *dcl1 dcl2* mutant was fully compromised in SIGS (Fig. 5AB).
255

bioRxiv preprint doi: https://doi.org/10.1101/633099; this version posted May 14, 2019. The copyright holder for this preprint (which was not certified by peer review) is the author/funder. All rights reserved. No reuse allowed without permission.

Discussion

We generated a broad collection of KO mutants in RNAi genes in the necrotrophic, mycotoxin-producing pathogen *Fusarium graminearum* (*Fg*) to demonstrate their involvement in vegetative and generative growth, FHB development and mycotoxin production. While all RNAi mutants show normal vegetative development in axenic cultures, there were differences in pigments production in liquid potato extract glucose cultures. This suggests that in *F. graminearum* an RNAi pathway regulates the gene cluster responsible for the biosynthesis of pigments, including aurofusarin. Aurofusarin is a secondary metabolite belonging to the naphthoquinone group of polyketides (Medentsev et al., 1998; Samson et al., 2000) that shows antibiotic properties against filamentous fungi and yeast (Medentsev et al., 1993). The function of the compound in the fungus is unresolved as white mutants have a higher growth rate than the wt and are as pathogenic on wheat and barley (Malz et al., 2005). Overall, the contribution of the RNAi pathways to vegetative fungal development varies strongly among different fungi and must be considered case by case. For instance, while the growth of *dcl* and *ago* mutants of the entomopathogenic *Metarhizium robertsii* was not affected (Meng et al., 2017), DCL2, on the contrary, regulates vegetative growth in *Trichoderma atroviride* (Carreras-Villaseñor et al., 2013).

Under low light (< 2 µmol m^{-2} s^{-1}) all RNAi mutants showed reduced conidia production and some also showed aberrant germination compared to IFA65 wt. This suggests that in absence of light induction the RNAi pathway is required for conidiation. RNAi may play a role in regulation of light responsive genes affecting conidiation as shown for *T. atroviride*, where DCL2 and RdRP3 control conidia production under light induction (Carreras-Villaseñor et al., 2013). The authors claimed that *Δdcl2* and *Δrdrp3* are impaired in perception and/or transduction of the light signal affecting the transcriptional response of light-responsive genes. *Metarhizium robertsii* DCL and AGO mutants show reduced abilities to produce conidia under light, though the light quantity was not described (Meng et al., 2017).

Perithecia development has been used to study sexual development and transcription of genes related to sexual development (Trail et al., 2000; Qi et al., 2006; Hallen et al., 2007). In field situations, ascospores serve as the primary inoculum for FHB epidemics because these spores are shot into the environment and can spread long distances (Maldonado-Ramirez et al., 2005). We found that all RNAi mutants could produce mature perithecia. However, corroborating and extending the exemplary work of Son et al. (2017), we also found that, beside *FgDCL1* and *FgAGO2*, other RNAi genes such as *RdRP1*, *RdRP2*, *RdRP3*, *RdRP4*, *QDE3*, *QIP* contribute

bioRxiv preprint doi: https://doi.org/10.1101/633099; this version posted May 14, 2019. The copyright holder for this preprint (which was not certified by peer review) is the author/funder. All rights reserved. No reuse allowed without permission.

to the sexual reproduction. Mutations in these genes either showed severe defect in forcible ascospore discharge or significantly reduced germination. The Son et al. study showed that the mutants *Fgdcl1* and *Fgago2* were severely defective in forcible ascospore discharge, while *Fgdcl2* and *Fgago1* showed indistinguishable phenotypes compared to the wt (Son et al., 2017). Active roles for FgDCL1 and FgAGO2 was supported by the finding that expression levels of many genes, including those closely related to the mating-type (*MAT*)-mediated regulatory mechanism during the late stages of sexual development, were compromised in the respective mutants after sexual induction (Kim et al., 2015). Moreover, FgDCL1 and FgAGO2 primarily participated in the biogenesis of sRNAs and perithecia-specific milRNAs also were dependent on FgDCL1 (Zeng et al. 2018). Most of the produced sRNA originated from gene transcript regions and affected expression of the corresponding genes at a post-transcriptional level (Son et al., 2017). We show

Here we show that, in addition to DCL1 and AGO2, also RdRP1, RdRP2, RdRP3, RdRP4, QIP and QDE3 are required for sex-specific RNAi, but further transcriptomic analysis and sRNA characterization are needed for a mechanistic explanation. Of note, ex-siRNA functions are important for various developmental stages and stress responses in the fungus *M. circinelloides*, while *F. graminearum* utilizes ex-siRNAs for a specific developmental stage. Thus, ex-siRNA-mediated RNAi might occur in various fungal developmental stages and stress responses depending on the fungal species.

We investigated the involvement of RNAi in pathogenicity and FHB development by infecting wheat spikes of the susceptible cultivar Apogee with fungal conidia. At earlier time points of infection (9 dpi) clear differences between RNAi mutants were observed, though all mutants could spread within a spike and caused typical FHB symptoms at later time points (13 dpi). Despite full FHB symptom development in all mutants at 13 dpi, we observed various effects of fungal infection on the kernel morphology, corresponding to the different aggressiveness of mutants at early time points. Since this phenomenon may account for differences in producing mycotoxins during infection, we quantified mycotoxins in the kernels. Of not, the relative amount of DON [rDON] as calculated as [DON] per amount of fungal genomic DNA was reduced in virtually all spikes infected with RNAi mutants, whereby [rDON] was strongly reduced especially in spikes colonized with mutants *Δago1*, *Δrdrp1*, *Δrdrp2*, *Δrdrp3*, *Δrdrp4* and *Δqde3* as compared with wt IFA65 (Tab. 2). The data suggest that fungal RNAi pathways affect *Fg*'s DON production in wheat spikes. While [rDON] changed, the ratio of [DON] and [3A-DON] remain constant in all mutants vs. IFA65, suggesting that the fungal RNAi pathways do not affect the trichothecene chemotype.

bioRxiv preprint doi: https://doi.org/10.1101/633099; this version posted May 14, 2019. The copyright holder for this preprint (which was not certified by peer review) is the author/funder. All rights reserved. No reuse allowed without permission.

In the present work, we also significantly extended the knowledge on the mechanism of SIGS-mediated control of plant diseases, a strategy, which might have great potential for more sustainable pesticide-reduced plant protections measures. We extended the earlier finding that DICER enzymes are required for gene silencing by hairpin or dsRNA in Fusarium (Chen et al., 2015; Koch et al., 2016). Of note, according to our data also AGO1 and AGO2 as well as QIP and RdRp1 are required for inhibiting *Fg* by exogenous dsRNA. More work is necessary to elucidate their specific roles in SIGS-mediated plant protection.

Taken together, our results further substantiate the involvement of RNAi pathways in conidiation, ascosporogenesis and pathogenicity of *Fusarium graminearum*. Further studies could explore the biological roles of *Fg* RNAi genes in sRNA production and processing during different developmental stages.

bioRxiv preprint doi: https://doi.org/10.1101/633099; this version posted May 14, 2019. The copyright holder for this preprint (which was not certified by peer review) is the author/funder. All rights reserved. No reuse allowed without permission.

Methods:

Fungal material, generation of gene deletion mutants in *Fusarium graminearum* (*Fg*)

The *Fg* strain PH1 and the PH1 *dcl1 dcl2* double mutant were a gift of Dr. Martin Urban, Rothamsted Research, England. RNAi gene deletion mutants were generated in the *Fg* strain IFA65 (Jansen et al. 2005). They were generated by homolog recombination using the pPK2 binary vector. *Fg* RNAi genes were identified by blasting *Neurospora crassa* genes against the Fusarium genome sequence in the Broad institute data base. Disruption vectors were constructed by inserting two flanking fragments (~1000 bp) upstream and downstream the corresponding genes in the pPK2 vector as follows: *RdRP1*, *AGO1*, *QDE3*, *QIP*, *AGO2*, *DCL1*, *RdRP2*, *RdRP3*, *RdRP4* and *DCL2* upstream flanking sequences were inserted in the plasmid between PacI- KpnI restriction sites, and the downstream flanking sequence were inserted between XbaI- HindIII restriction sites. Except *AGO2* downstream flanking sequence was inserted in XbaI restriction site (primers used in disruption plasmid construction are listed in Table S1. Disruption vectors were introduced into Agrobacterium (LBA440 and AGL1 strains) by electroporation. A single colony of Agrobacterium containing the pPK2 plasmid were grown in 10 ml YEB medium (Vervliet et al., 1975) containing the appropriate antibiotics (5 µg/ml tetraciclin + 25 µg/ml rifampicin + 50 µg/ml Kanamycin for LBA440, and 25 µg/ml carbenicillin + 25 µg/ml rifampicin + 50 µg/ml kanamycin for AGL1) and were incubated at 28ºC till OD_{600nm} was reached 0.7. Then T-DNA was mobilized in Agrobacterium with 200 µM acetosyringone (Utermark et al., 2008), and the *Agrobacterium tumefaciens* and fungal recipient were co-cultivated on black filter paper (DP 551070, Albert LabScience, Hahnemühle, Dassel, Germany), respectively. Putative *Fg* IFA65 mutants were selected on potato extract glucose medium containing 150 µg/ml hygromycin + 150 µg/ml ticarcillin and grown for five days. For genotyping, genomic DNA of putative Fusarium mutants were extracted from mycelia.

Genotyping of Fusarium mutants

Fg IFA65 mutants were confirmed by genotyping using primers located in Hygromycin and corresponding genes flanking sequence (located after the cloned flanking sequence in the genome), and primers amplify parts of the genes (Table S2) and sequenced, respectively. Additionally, mRNA expression of the deleted gene in comparison to that in the wild type (IFA65 strain) was done by qRT-PCR using primers pairs listed in (Table S3). The mRNA transcripts were measured using 1 x SYBR Green JumpStart Taq Ready Mix (Sigma-Aldrich) according to manufacturer's instructions and assayed in 7500 Fast Real-Time PCR cycler

bioRxiv preprint doi: https://doi.org/10.1101/633099; this version posted May 14, 2019. The copyright holder for this preprint (which was not certified by peer review) is the author/funder. All rights reserved. No reuse allowed without permission.

(Applied Biosystems Inc, CA, USA) under the following thermal cycling conditions: initial activation step at 95 °C for 5 min, 40 cycles (95°C for 30 s, 53°C for 30 s, and 72°C for 30 s). The Ct values were determined with the software in the qRT-PCR instrument and the transcript levels of the genes was determined according to the $2^{-\Delta\Delta Ct}$ method (Livak and Schittgen, 2001).

Colony morphology

The RNAi mutants were cultured in plates of potato extract glucose (ROTH, Germany); starch agar and Synthetic Nutrient Agar (SNA) media (Leslie and Summerell, 2006). The plates were incubated at 25ºC in 12h light/12h dark (52µmol m^{-2} s^{-1}, Philips Master TL-D HF 16W/840). The growth was documented after 5 days.

Growth morphology in liquid medium

Agar blocks from 2-week-old fungal cultures were incubated on liquid PEG medium for five days at RT, light (2 µmol m^{-2} s^{-1}) with shaking. Each mutant was grown in flask containing medium supplemented with hygromycin (100 µg/ml) and flask containing medium without hygromycin. Photos were taken to document the growth pattern after five days incubation.

Production of fungal biomass

Fifty milligram mycelia (fresh mycelia from four-day-old fungal cultures grown in Aspergillus Complete Medium (CM) plates in dark (Leslie and Summerell, 2006) were incubated in a 100 ml flask containing 20 ml of PEG medium incubated at RT with shaking under 12 h light (2 µmol m^{-2} s^{-1}). Fungal mycelium was harvested after 3 days growth by filtration through filter paper (Munktell, AHLSTROM, Germany GMBH) and washed with distilled water twice and dried at 75°C overnight. The dry weight was calculated by using the following formula: Dry weight = (weight of filter paper + mycelium) - (weight of filter paper).

Conidiation assay

Production of conidia was done with slight modification (Yun et al., 2015). Four-day-old cultures of each mutant and IFA65 (wt) growing in CM agar plates in dark at 25°C were used for fresh mycelia preparation. The mycelia were scraped from plates surface using sterile toothpick, then 50 mg mycelia were inoculated in a 100 ml flask containing 20 ml of synthetic nutrient (SN) medium. The flasks were incubated at room temperature for 5 days in light (2 µmol m^{-2} s^{-1}) in a shaker (100 rpm). Subsequently, the conidia produced from each mutant and

bioRxiv preprint doi: https://doi.org/10.1101/633099; this version posted May 14, 2019. The copyright holder for this preprint (which was not certified by peer review) is the author/funder. All rights reserved. No reuse allowed without permission.

wild type was counted using a hemocytometer (Fuchs Rosenthal, Superior Marienfeld, Germany).

Viability test of conidia

Fourteen mL from the same cultures used in conidiation assay was centrifuged in 4,000 rpm for 10 min to precipitate conidia, and then the conidia was resuspended in 5 ml 2% sucrose water and incubated in dark for 2 days at 23°C. The germinated and non-germinated ascospores were visualized and counted under an inverse microscope. Conidia germination rate was determined as percentage of germinated conidia of the total conidia number.

Perithecia production and ascospore discharge assay

Fungi were grown on carrot agar prepared under bright fluorescent light at room temperature (18-24°C) for five days (Klittich and Leslie, 1988). Then the aerial mycelia were removed with a sterile tooth stick. To stimulate sexual reproduction and perithecia formation, one ml of 2.5% Tween 60 was applied to the plates with a sterile glass rod after scraping the mycelia (Cavinder et al., 2012). The plates were incubated under fluorescent light at RT for nine days. Subsequently, agar blocks (1.5 cm in diameter) were cut from the plates containing the mature perithecia using a cork borer. Agar blocks were sliced in half, placed on glass microscope slides, and incubated in boxes under high humidity for two days under 24 h light (52 µmol m^{-2} s^{-1} Philips Master TL-D HF 16W/840). During this time, ascospores discharged from the perithecia accumulated on the slide. For the quantification of discharged ascospores, slides were washed off by 2 ml of an aqueous Tween 20 (0.002%) solution and counted using a hemocytometer.

Viability test of the discharged ascospores

Mycelia with mature perithecia (13 days after sexual induction) on carrot agar were incubated in a humid box at room temperature under lights for 4 days according to (Son et al., 2017). The discharged ascospores were washed from plates cover using SN liquid medium and were incubated in dark for 24 h in a humid box. The germinated and non-germinated ascospores were visualized under an inverse microscope and counted.

Pathogenicity assay on wheat ears

The susceptible wheat cultivar Apogee was used. Plants were grown in an environmentally controlled growth chamber (24°C, 16 h light, 180 µmol m^{-2} s^{-1} photon flux density, 60% rel. humidity) till the anthesis. Point inoculations to the second single floret of each spike were

bioRxiv preprint doi: https://doi.org/10.1101/633099; this version posted May 14, 2019. The copyright holder for this preprint (which was not certified by peer review) is the author/funder. All rights reserved. No reuse allowed without permission.

performed at mid-anthesis with 5 µL of a 40,000 conidia/mL suspension amended with 0.002% v/v Tween 20 (Gosman et al., 2010).

Control plants were inoculated with sterile 0.002% v/v Tween 20. For each *Fg* genotype, ten wheat heads were inoculated and incubated in plastic boxes misted with water to maintain high humidity for two days. Then incubation continued at 22°C at 60% rel. humidity. Infected wheat heads were observed 11 and 13 dpi and infection percentage was determined as the ratio of infected spikelets to the total spikelet number per ear.

Thousand Grain Weight (TGW) of infected wheat kernels

Hundred kernels from two biological experiments with 10 wheat heads point-inoculated with wt IFA65 and mutants were counted and weighed. TGW was calculated in grams per 1000 kernels of cleaned wheat seeds.

Quantification of fungal DNA in infected wheat kernels

Fungal genomic DNA in kernels was quantified using qPCR as described (Brandfass and Karlovsky, 2008). Dried grains were ground. DNA was extracted from 30 mg flour and dissolved in 50 µl of TE buffer. One µl of 50x diluted DNA was used as template for real-time PCR with primers amplifying 280 bp fragment specific for *F. graminearum*. The PCR mix consisted of reaction buffer (16 mM $(NH_4)_2SO_4$, 67 mM Tris–HCl, 0.01% Tween-20, pH 8.8 at 25°C; 3 mM $MgCl_2$, 0.3 µM of each primer, 0.2 mM of each dATP, dTTP, dCTP and dGTP (Bioline), 0.03 U/µl Taq DNA polymerase (Bioline, Luckenwalde, Germany) and 0.1x SYBR Green I solution (Invitrogen, Karlsruhe, Germany). The PCR was performed in CFX384 thermocycler (BioRad, Hercules, CA, USA) according to the following cycling condition: Initial denaturation 2 min at 95°C, 35 cycles with 30 s at 94°C, 30 s at 61°C, 30 s at 68°C, and final elongation for 5 min at 68°C. No matrix effects were detectable with 50-fold diluted DNA extracted from grains. Standards were prepared from pure *Fg* DNA in 3-fold dilution steps from 100 pg to 0.4 pg/well.

Analysis of mycotoxins in infected wheat kernels

The content of mycotoxins in wheat kernels infected with *Fg* RNAi mutants and wild type strain IFA65 was determined using high performance liquid chromatography coupled to tandem mass spectrometry (HPLC–MS/MS). Mycotoxins were extracted from ground grains with mixture containing 84% acetonitrile, 15% water and 1% acetic acid and the extracts were defatted with cyclohexane. Chromatographic separation was carried out on a C18 column eluted with a

bioRxiv preprint doi: https://doi.org/10.1101/633099; this version posted May 14, 2019. The copyright holder for this preprint (which was not certified by peer review) is the author/funder. All rights reserved. No reuse allowed without permission.

water/methanol gradient and the analytes were ionized by electrospray and detected by MS/MS in multiple reaction monitoring (MRM) mode essentially as described (Sulyok et al., 2006).

Spray application of dsRNA on barley leaves

Second leaves of 3-week-old barley cultivar Golden Promise were detached and transferred to square Petri plates containing 1% water-agar. dsRNA spray applications and leaf inoculation was done virtually as described (Koch et al. 2016). For the TE-control, TE-buffer was diluted in 500 µl water corresponding to the amount used for dilution of the dsRNA. Typical RNA concentration after elution was 500 ng μl^{-1}, representing a buffer concentration of 400 µM Tris-HCL and 40 µM EDTA in the final dilution. TE buffer were indistinguishable from treatments with control dsRNA generated from the GFP or GUS gene, respectively (Koch et al., 2016; Koch et al., 2018). Thus, we used TE buffer as control to save costs. Spraying of the leaves was carried out in the semi-systemic design (Koch et al. 2016), where the lower parts of the detached leaf segments were covered by a tinfoil to avoid direct contact of dsRNA with the leaf surface that was subsequently inoculated.

Statistics and analysis

Data obtained from two or three repetitions were subjected to the Student's *t* test in Microsoft office Excel 2010. Significance was determined as $P \leq 0.05$, 0.01 or 0.001 and indicated by *, ** or ***, respectively. Unless specified otherwise, data are presented as mean ± standard error or mean ± standard deviation of the mean. Sequence analysis was performed on the ApE plasmid editor free tool. Basic Local Alignment Search Tool (BLAST) NCBI BLAST (http://blast.ncbi.nlm.nih.gov/Blast.cgi) was used for sequences search and alignment.

List of abbreviations

AGO, Argonaute

CYP51, *Cytochrome P450 lanosterol C-14α-demethylase*

DCL, Dicer-like

DON, deoxynivalenol

Fg, *Fusarium graminearum*

FHB, Fusarium head blight

HIGS, host-induced gene silencing

hpRNA, hairpin RNA

bioRxiv preprint doi: https://doi.org/10.1101/633099; this version posted May 14, 2019. The copyright holder for this preprint (which was not certified by peer review) is the author/funder. All rights reserved. No reuse allowed without permission.

MSUD, meiotic silencing by unpaired DNA
NIV, nivalenol
PEG, potato extract glucose
QDE 2,3, Quelling defective 2,3
QIP, QDE-interacting protein
RdRp, RNA-dependent RNA polymerase
RISC, RNA-dependent silencing complex,
RNAi, RNA interference
RPA, subunit of replication protein A
siRNA, small interfering RNA
SNA, synthetic nutrient agar
ssDNA, single-stranded
TGW, thousand grain weight

Declarations

Ethics approval and consent to participate

Not applicable

Consent for publication

Not applicable

Availability of data and material

All data generated or analysed during this study are included in this published article [and its supplementary information files].

Competing interests

The authors declare that they have no competing interests" in this section.

Funding

This research was supported by the German Research Council (DFG) to K.-H. K in the project GRK2355

Authors' contributions

FYG and JI conducted the experimental work; JI and KHK designed the research and wrote the manuscript. PK conducted the experiments related to *Fg* mycotoxins.

Acknowledgements

bioRxiv preprint doi: https://doi.org/10.1101/633099; this version posted May 14, 2019. The copyright holder for this preprint (which was not certified by peer review) is the author/funder. All rights reserved. No reuse allowed without permission.

We thank Mrs. E. Stein for excellent technical assistance, Dr. A. Rathgeb for mycotoxin analysis and Ms. C. Birkenstock for caring of the plants. The *Fg* strain PH1 and the PH1 *dcl1 dcl2* double mutant were a kind gift of Dr. Martin Urban, Rothamsted Research, England.

bioRxiv preprint doi: https://doi.org/10.1101/633099; this version posted May 14, 2019. The copyright holder for this preprint (which was not certified by peer review) is the author/funder. All rights reserved. No reuse allowed without permission.

Legends to figures

Fig. 1. PCR verification of targeted gene replacement in *Fusarium graminearum*. (A) Amplification of an internal part of the targeted genes *DCL1*, *DCL2*, *AGO1*, *AGO2*, *RdRP1*, *RdRP4*, *RdRP2*, *RdRP3*, *QIP*, and *QDE3* are positive in the IFA65 (wt) strain and negative in corresponding mutants. (**B)** PCR with primer pairs in the right recombination sequence and hygromycin, showing that the antibiotic resistance gene had integrated into the target gene locus. PCR products were analyzed on 1.5% agarose gel electrophoresis. M; DNA marker. wt; wild type.

Fig. 2. The RNAi pathway is required for asexual development of *Fusarium graminearum* in the absence of inductive light. (A) Number of conidia produced: Means± SEs of the percentage of conidia numbers from three repeated experiments. Significant differences are marked: *P, 0.05, **P, 0.01, ***P, 0.001 (Student's *t* test). **(B)** Percent of conidial germination: Means± SEs of the percentage of germinated spores from three biological repetitions. Significant differences are marked: *P, 0.05 (Student's t test). **(C)** Microscopic observation of germinated and non-germinated conidia of IFA65 (wt) and *Δrdrp4*. Imaging after 48 h incubation in dark, scale bar: 50 µm. Black arrow; conidia forming a bipolar germ tube. Red arrow; conidia forming multiple germ tubes.

Fig. 3. Forcible ascospore discharge in *Fusarium graminearum* RNAi mutants and wt strain IFA65. (A) Forcible ascospore firing. Half circular carrot agar blocks covered with mature perithecia were placed on glass slides. Photos from forcibly fired ascospores (white cloudy) were taken after 48 h incubation in boxes under high humidity and fluorescent light. **(B)** Fired ascospores were washed off and counted. Means± SDs of the counted spores is presented from three biological repetitions. Significant differences are marked: *P, 0.05, ***P, 0.001 (Student's t test). **(C)** Ascospore germination. Discharged ascospores were incubated at 100% relative humidity in the dark for 24 h at 23°C in SN liquid medium. The percentage of germination was assessed by examining the ascospore number in three random squares in the counting chamber. Means± SEs of the percentage of germinated spores from three biological repetitions. Significant differences are marked: *P, 0.05 (Student's t test).

Fig. 4. Infection of wheat spikes with *Fusarium graminearum* RNAi mutants and wt strain IFA65. (A) Representative samples of spikes at 9 and 13 dpi. One spikelet at the bottom of each

bioRxiv preprint doi: https://doi.org/10.1101/633099; this version posted May 14, 2019. The copyright holder for this preprint (which was not certified by peer review) is the author/funder. All rights reserved. No reuse allowed without permission.

spike (red arrow) was point inoculated with 5 µl of 0.002% Tween 20 water containing 40,000 conidia / mL. The assay was repeated two times with 10 spikes per fungal genotype and experiment. **(B)** Wheat kernels 13 dpi with *Fg* RNAi mutants and wt strain IFA65.

Fig. 5 Infection symptoms of *Fg* RNAi mutants on barley leaves sprayed with CYP3RNA. **A.** Detached leaves of 3-week-old barley plants were sprayed with 20 ng μl^{-1} CYP3RNA or TE buffer, respectively. After 48 h, leaves were drop-inoculated with 5 x 10^4 conidia ml^{-1} of indicated *Fg* RNAi mutants and evaluated for infection symptoms at 5 dpi. Values show relative infection area as calculated from TE- vs. CYP3RNA-treated plants for each RNAi mutant with 10 leaves and thee biological repetitions. Asterisks indicate statistical significant reduction of the infection area on CYP3RNA- vs. TE-treated plants measured by ImageJ for each mutant (**p<0,01; ***p< 0,001; students t-test). The *dcl1 dcl2* double mutant is generated in *Fg* strain PH1. (**B**). Downregulation of the three *CYP51* genes in *Fg* mutants upon colonization of CYP3RNA- vs. TE-treated barley leaves. Strong down-regulation of all three *CYP51* genes is only observed in both *Fg* wild-types and in the mutant *Δqde3*. Asterisks indicate statistical significant downregulation of *CYP51* genes on CYP3RNA vs. TE-treated plants. (**p<0,01; ***p< 0,001; students t-test). Error bars indicate SE of three independent experiments in A and B.

References

Alexander, W.G., Raju, N.B., Xiao, H., Hammond, T.M., Perdue, T.D., Metzenberg, R.L., et al. (2008). DCL-1 colocalizes with other components of the MSUD machinery and is required for silencing. Fungal Genet Biol. 45(5):719-727.

Audenaert, K., Vanheule, A., Höfte, M., Haesaert, G. (2014). Deoxynivalenol: A Major Player in the Multifaceted Response of Fusarium to Its Environment. Toxins (Basel). doi: 10.3390/toxins6010001.

Bai, Y., Lan, F., Yang, W., Zhang, F., Yang, K., Li, Z. et al. (2015). sRNA profiling in Aspergillus flavusreveals differentially expressed miRNA-like RNAs response to water activity and temperature. Fungal Genet Biol. 81:113-119.

Baulcombe, D.C. (2013). Small RNA-the Secret of Noble Rot. Science. doi: 10.1126/science.1245010.

Brandfass, C., and Karlovsky, P. (2008). Upscaled CTAB-Based DNA Extraction and Real-Time PCR Assays for *Fusarium culmorum* and *F. graminearum* DNA in Plant Material with Reduced Sampling Error. Int J Mol Sci.;doi: 10.3390/ijms9112306.

Brown, N., Evans, A.J., Mead, A., and Hammond-Kosack, K.E. (2017). A spatial temporal analysis of the *Fusarium graminearum* transcriptome during symptomless and symptomatic wheat infection. Mol Plant Pathol 18 (9).

Cai, Q., He, B., Kogel, K.H., and Jin, H. (2018). Cross-kingdom RNA trafficking and environmental RNAi — nature's blueprint for modern crop protection strategies. Curr Opin Microbiol. doi:10.1016/j.mib.2018.02.003.

bioRxiv preprint doi: https://doi.org/10.1101/633099; this version posted May 14, 2019. The copyright holder for this preprint (which was not certified by peer review) is the author/funder. All rights reserved. No reuse allowed without permission.

612 Calo, S., Nicolás, F.E., Vila, A., Torres-Martínez, S., and Ruiz-Vázquez, R.M. (2012). Two distinct
613 RNA-dependent RNA polymerases are required for initiation and amplification of RNA silencing in the
614 basal fungus Mucor circinelloides. Mol Microbiol. 83.

615 Campo, S., Gilbert, K.B., and Carrington, J.C. (2016). Small RNA-based antiviral defense in the
616 phytopathogenic fungus *Colletotrichum higginsianum*. PLoS Pathog. doi:
617 10.1371/journal.ppat.1005640.

618 Carreras-Villaseñor, N., Esquivel-Naranjo, E.U., Villalobos-Escobedo, J.M., Abreu-Goodger, C., and
619 Herrera-Estrella, A. (2013). The RNAi machinery regulates growth and development in the filamentous
620 fungus Trichoderma atroviride. Mol Microbiol. doi:10.1111/mmi.12261.

621 Cavinder, B., Sikhakolli, U., Fellows, K.M., Trail, F. (2012). Sexual development and ascospore
622 discharge in *Fusarium graminearum*. J Vis Exp. doi: 10.3791/3895.

623 Chang SS, Zhang Z, and Liu Y. (2012). RNA interference pathways in fungi: mechanisms and functions.
624 Annu Rev Microbiol. 66.

625 Chen., Y, Gao, Q., Huang, M., Liu, Y., Liu, .Z, Liu X., and Ma, Z. (2015). Characterization of RNA
626 silencing components in the plant pathogenic fungus *Fusarium graminearum*. Sci Rep. doi:
627 10.1038/srep12500.

628 Cogoni C, and Macino G. (1999). Gene silencing in Neurospora crassa requires a protein homologous
629 to RNA-dependent RNA polymerase. Nature. 399(6732):166-9.

630 Cuomo, C.A., Güldener, U., Xu, J.R., Trail, F., Turgeon, B.G., Di Pietro A., et al. (2007). The *Fusarium*
631 *graminearum* genome reveals a link between localized polymorphism and pathogen specialization.
632 Science. 317.

633 Dalakouras A, Wassenegger M, McMillan J.N., Cardoza V., Maegele, I, Dadami E., Runne M, Krczal
634 G and Wassenegger MK (2016). Induction of Silencing in Plants by High-Pressure Spraying of *In vitro*-
635 Synthesized Small RNAs. Front. Plant Sci., doi.org/10.3389/fpls.2016.01327

636 Dang Y, Yang Q, Xue Z, and Liu Y. (2011). RNA Interference in Fungi: Pathways, Functions, and
637 Applications. Eukaryot. Cell. 10.

638 Dean, R., Van Kan, J.A., Pretorius, Z.A., Hammond-Kosack K.E., Di Pietro, A., Spanu, P.D., Rudd,
639 J.J., Dickman, M., Kahmann, R., Ellis J., and Foster G.D. (2012). The top 10 fungal pathogens in
640 molecular plant pathology. Mol Plant Pathol. doi: 10.1111/j.1364-3703.2011.00783.x.

641 Desjardins AE, Hohn TM, and McCormick SP. (1993). Trichothecene biosynthesis in Fusarium species:
642 Chemistry, genetics and significance. Microbiol Rev. 57.

643 Dill-Macky R, and Jones RK. (2000). The effect of previous crop residues and tillage on Fusarium head
644 blight of wheat. Plant Dis. 2000;84.

645 Fire A, Xu, S, Montgomery, MK, Kostas, SA, Driver, SE, and Mello, CC. (1998). Potent and specific
646 genetic interference by double-stranded RNA in *Caenorhabditis elegans*. Nature. 391.

647 Frandsen, R.J., Nielsen, N.J., Maolanon, N., Sørensen, J.C., Olsson, S., Nielsen, J., and Giese, H. (2006).
648 The biosynthetic pathway for aurofusarin in *Fusarium graminearum* reveals a close link between the
649 naphthoquinones and naphthopyrones. Mol Microbiol. 61(4).

650 Gosman, N., Steed, A., Chandler, E., Thomsett, M., Nicholson, P. (2010). Evaluation of type I fusarium
651 head blight resistance of wheat using non-deoxynivalenol-producing fungi. Plant Pathology 147 (59).

652 Hallen H, Huebner M, Shiu SH, Guldener U, and Trail F. (2007). Gene expression shifts during
653 perithecium development in *Gibberella zeae* (anamorph *Fusarium graminearum*), with particular
654 emphasis on ion transport proteins Fungal Genet Biol. 44.

655 Hammond, S.M. (2005). Dicing and slicing: the core machinery of the RNA interference pathway. FEBS
656 Lett. 579 (26).

bioRxiv preprint doi: https://doi.org/10.1101/633099; this version posted May 14, 2019. The copyright holder for this preprint (which was not certified by peer review) is the author/funder. All rights reserved. No reuse allowed without permission.

Harris, L.J, Balcerzak, M., Johnston, A,. Schneiderman, D., and Ouellet, T. (2016). Host-preferential *Fusarium graminearum* gene expression during infection of wheat, barley, and maize. Fungal Biol. 120 (1).

Ilgen, P., Hadeler, B., Maier, F.J., and Schäfer, W. (2009). Developing kernel and rachis node induce the trichothecene pathway of *Fusarium graminearum* during wheat head infection. Mol Plant Microbe Interact. 22.

Jansen, C., von Wettstein, D., Schäfer, W., Kogel, K.H., Felk, F., and Maier, F.J. (2005). Infection patterns in barley and wheat spikes inoculated with wild type and trichodiene synthase gene disrupted *Fusarium graminearum.* Proc. Nat. Acad. Sci USA. 102.

Kim, HK, Jo, SM, Kim, GY, Kim DW, Kim, YK, and Yun, SH. (2015). A large-scale functional analysis of putative target genes of mating-type loci provides insight into the regulation of sexual development of the cereal pathogen *Fusarium graminearum*. PLoS Genet. 11.

Klittich, C,J,R, and Leslie, J,F. (1988). Nitrate reduction mutants of *Fusarium moniliforme* (*Gibberella fujikuroi*). Genetics. 118.

Koch, A., Biedenkopf, D., Furch, A., Weber, L., Rossbach O., Abdellatef E., Linicus, L., Johannsmeier, J., Jelonek, L., Goesmann, A., Cardoza V., McMillan, J., Mentzel, T., and Kogel, K.H. (2016). An RNAi-Based Control of *Fusarium graminearum* infections through spraying of Long dsRNAs involves a plant passage and is controlled by the fungal silencing machinery. PLoS Pathog doi:10.1371/journal.ppat.1005901.

Koch, A., and Kogel, K.H. (2014). New wind in the sails: improving the agronomic value of crop plants through RNAi-mediated gene silencing. Plant Biotechnol J. doi: 10.1111/pbi.12226.

Koch, A., Kumar, N., Weber, L., Keller, H., Imani, J., and Kogel, K.H. (2013). Host-induced gene silencing of cytochrome P450 lanosterol C14α-demethylase–encoding genes confers strong resistance to Fusarium species. Proc Natl Acad Sci U S A. doi: 10.1073/pnas.1306373110.

Koch A, Stein E, and Kogel KH (2018). RNA-based disease control as a complementary measure to fight Fusarium fungi through silencing of the Azole target cytochrome P450 lanosterol C-14 α-demethylase. Eu. J Plant Pathol. DOI 10.1007/s10658-018-1518-4.

Kusch, S., Frantzeskakis, L., Thieron, H., and Panstruga, R. (2018). Small RNAs from cereal powdery mildew pathogens may target host plant genes. Fungal Biol. doi.org/10.1016/j.funbio.2018.08.008.

Lau, S.K., Tse, H., Chan, J.S., Zhou, A.C., Curreem, S.O., Lau, C.C., Yuen, K.Y., and Woo, P.C. (2013). Proteome profiling of the dimorphic fungus *Penicillium marneffei* extracellular proteins and identification of glyceraldehyde-3-phosphate dehydrogenase as an important adhesion factor for conidial attachment. FEBS J. doi: 10.1111/febs.12566.

Lee, D.W., Pratt, R.J., McLaughlin, M., and Aramayo, R. (2003). An Argonaute-like protein is required for meiotic silencing. Genetics.164.

Leslie, J.F., Summerell, B.A. (2006) The Fusarium laboratory manual. Blackwell Professional, Ames, IA, USA; .

Livak, K.J., Schmittgen, T.D. (2001). Analysis of relative gene expression data using real-time quantitative PCR and the 2ΔΔC(T) Method. Methods. 25 (4).

Maldonado-Ramirez SL, Schmale DG, Jr Shields EJ, Bergstrom GC. (2005). The relative abundance of viable spores of *Gibberella zeae* in the planetary boundary layer suggests the role of long-distance transport in regional epidemics of Fusarium head blight. Agric For Meteorol. doi: 10.1016/j.agrformet.2005.06.007.

Malz, S., Grell, M.N., Thrane, C., Maier, F.J., Rosager, P., Felk, A., Albertsen, K.S., Salomon, S., Bohn L., Schäfer, W., and Giese, H. (2005). Identification of a gene cluster responsible for the biosynthesis of aurofusarin in the *Fusarium graminearum* species complex. Fungal Genet Biol. doi:10.1016/j.fgb.2005.01.010.

bioRxiv preprint doi: https://doi.org/10.1101/633099; this version posted May 14, 2019. The copyright holder for this preprint (which was not certified by peer review) is the author/funder. All rights reserved. No reuse allowed without permission.

McLoughlin, A.G., Wytinck, N., Walker, P.L., Girard, I.J., Rashid, K.Y., de Kievit, T., Dilantha, W.G. Fernando, Whyard, S. and Belmonte, M.F. (2018) 1Identification and application of exogenous dsRNA confers plant protection against Sclerotinia sclerotiorum and Botrytis cinerea. Scientific Reports 8:7320 DOI:10.1038/s41598-018-25434-4.

Medentsev, A.G., Kotik, A.N., Trufanova, V.A., and Akimenko, V.K. (1993). Identification of aurofusarin in *Fusarium graminearum* isolates, causing a syndrome of worsening of egg quality in chickens. Prikl Biokhim Mikrobiol. 29.

Mello, C.C., and Conte, D, Jr. (2004). Revealing the world of RNA interference. Nature 431.

Meng, H, Wang, Z, Wang, Y, Zhu, H and Huang, B. (2017). Dicer and Argonaute genes involved in RNA interference in the entomopathogenic fungus *Metarhizium robertsii*. Appl. Environ. Microbiol. doi: 10.1128/AEM.0323016.

Nguyen, Q., Iritani, A., Ohkita, S., Vu, B.V., Yokoya, K., Matsubara, A., Ikeda, K.I., Suzuki, N., Nakayashiki, H. (2018). A fungal Argonaute interferes with RNA interference. Nucleic Acids Res. 16;46(5).

Nowara, D., Gay, A., Lacomme, C., Shaw, J., Ridout, C., Douchkov, D., Hensel, G., Kumlehn, J., and Schweizer, P. (2010). HIGS: Host-induced gene silencing in the obligate biotrophic fungal pathogen *Blumeria graminis*. Plant Cell. doi: https://doi.org/10.1105/tpc.110.077040.

Qi, W., Kwon C., and Trail, F. (2006). Microarray analysis of transcript accumulation during perithecium development in *Gibberella zeae* (anamorph *Fusarium graminearum*). Mol Genet Genomics 276(1):87-100.

Raman, V., Simon, S.A., Demirci, F., Nakano, M., Meyers, B.C., and Donofrio, N.M. (2017) Small RNA functions are required for growth and development of *Magnaporthe oryzae*. Mol Plant Microbe Interact. 30(7).

Romano, N., and Macino, G. (1992). Quelling: transient inactivation of gene expression in *Neurospora crassa* by transformation with homologous sequences. Mol Microbiol.6.

Samson, R.A., Frisvad, J.C., Hoekstra, E.S. (2000). Introduction to Food- and Airborn Fungi, 6th edn. Utrecht, NL: Centraalbureau voor Schimmelcultures.

Segers, G.C., Zhan,g X., Deng, F., Sun, Q., Nuss, D.L. (2007). Evidence that RNA silencing functions as an antiviral defense mechanism in fungi. Proc Natl Acad Sci USA. 104.

Shiu, P.K., Raju, N.B., Zickler, D., Metzenberg, R.L. (2001). Meiotic silencing by unpaired DNA. Cell. 107.

Son, H., Min, K., Lee, J., Raju, N.B., and Lee, Y.W. (2011). Meiotic silencing in the homothallic fungus *Gibberella zeae*. FUNGAL BIOL-UK. 115.

Son, H., Park, A.R., Lim, J.Y., Shin, C., and Lee, Y.W. (2017). Genome-wide exonic small interference RNA-mediated gene silencing regulates sexual reproduction in the homothallic fungus *Fusarium graminearum*. PLoS Genet. doi.org/10.1371/journal.pgen.1006595.

Song, M.S., and Rossi, J.J. (2017). Molecular mechanisms of Dicer: endonuclease and enzymatic activity. Biochem J. 474(10).

Sulyok, M., Berthiller, F., Krska, R., and Schuhmacher, R. (2006). Development and validation of a liquid chromatography/tandem mass spectrometric method for the determination of 39 mycotoxins in wheat and maize. Rapid Commun Mass Spectrom. 20.

Torres-Martínez, S., and Ruiz-Vázquez, R.M. (2017). The RNAi universe in fungi: A varied landscape of small RNAs and biological functions. Annu Rev Microbiol. 71.

Trail, F., and Common, R. (2000). Perithecial development by *Gibberella zeae*: a light microscopy study. Mycologia. 92.

bioRxiv preprint doi: https://doi.org/10.1101/633099; this version posted May 14, 2019. The copyright holder for this preprint (which was not certified by peer review) is the author/funder. All rights reserved. No reuse allowed without permission.

749 Urban, M., King, R., Hassani-Pak, K., and Hammond-Kosack, K.E. (2015). Whole-genome analysis of
750 *Fusarium graminearum* insertional mutants identifies virulence associated genes and unmasks untagged
751 chromosomal deletions. BMC Genomics. doi: 10.1186/s12864-015-1412-9.

752 Utermark, J., and Karlovsky, P. (2008). Genetic transformation of filamentous fungi by *Agrobacterium*
753 *tumefaciens*. Nat. Protoc. 2008; doi:10.1038/nprot.2008.83.

754 Vervliet, G., Holsters, M., Teuchy, H., Van Montagu, M., and Schell, J. (1975). Characterization of
755 different plaque-forming and defective temperate phages in Agrobacterium strains. J Gen Virol. 26.

756 Wang, S., Li P., Zhang, J., Qiu, D., and Guoa, L. (2016). Generation of a high resolution map of sRNAs
757 from *Fusarium graminearum* and analysis of responses to viral infection. Scientific Reports. doi:
758 10.1038/srep26151.

bioRxiv preprint doi: https://doi.org/10.1101/633099; this version posted May 14, 2019. The copyright holder for this preprint (which was not certified by peer review) is the author/funder. All rights reserved. No reuse allowed without permission.

759 Wang, M., Weiberg, A., Lin, F.M., Thomma, B.P., Huang, H.D., and Jin, H. (2016). Bidirectional cross-
760 kingdom RNAi and fungal uptake of external RNAs confer plant protection. Nature plants *2*, 16151.

761 Weiberg A, Wang M, Lin F-M, Zhao H, Zhang Z, et al. Fungal Small RNAs Suppress Plant Immunity
762 by Hijacking Host RNA Interference Pathways. Science. 2013;doi: 10.1126/science.1239705.

763 Yun Y, Liu Z, Yin Y, Jiang J, Chen Y, Xu JR, Ma Z. Functional analysis of the *Fusarium graminearum*
764 phosphatome. New Phytol. 2015; doi: 10.1111/nph.13374.

765 Zanini S, Šečić E, Jelonek L, Kogel KH (2018) A bioinformatics pipeline for the analysis and target
766 prediction of RNA effectors in bidirectional communication during plant-microbe interactions. Front.
767 Plant Sci. doi: 10.3389/fpls.2018.01212.

768 Zeng W., Wang J, Wang Y, Lin J, Fu Y, Xie J, Jiang D, Chen T, Liu H and Cheng J. (2018) Dicer-Like
769 Proteins Regulate Sexual Development via the Biogenesis of Perithecium-Specific MicroRNAs in a
770 Plant Pathogenic Fungus *Fusarium graminearum. Frontiers in Microbiology*. doi:
771 10.3389/fmicb.2018.00818

772 Zhang H, Xia R, Meyers BC, Walbot V. Evolution, functions, and mysteries of plant ARGONAUTE
773 proteins. Curr Opin Plant Biol. 2015;27.

774 **Table 1**: RNAi pathway genes of *Fusarium graminearum* (*Fg*) as identified from
775 www.Broadinstitute.org and used in this study.

776

RNAi proteins in *Neurospora crassa*	**Homologs in *Fg***	**aa identity (%)**	**Fusarium gene ID**	**Gene function in *Fg***
DICER1	*Fg*DCL1	43%	FGSG_09025	Antiviral defence (Wang et al., 2016). Minor role in processing of exogenous dsRNA, hpRNA or pre-milRNA in mycelium (Chen et al., 2015). Major role in sex-specific RNAi pathway: Production of regulatory sRNAs. Required for ascospore production (Son et al., 2017).
DICER2	*Fg*DCL2	35%	FGSG_04408	Processing of exogenous dsRNA, hpRNA and pre-milRNA in mycelium (Chen et al., 2015). Partially shared DCL-1 role in production of regulatory sRNAs in the sexual stage (Son et al., 2017).
ARGONAUTE1 (syn. Quelling defective 2)	*Fg*AGO1	59%	FGSG_08752	Major component in the RISC during quelling (Chen et al., 2015).
ARGONAUTE2 (syn. Suppressor of meiotic silencing2, SMS2)	*Fg*AGO2	43%	FGSG_00348	Minor role in binding siRNA derived from exogenous dsRNA, hpRNA or pre-milRNA in mycelium (Chen et al., 2015). Major role in sex-specific RNAi pathway; required for ascospore production (Son et al., 2017).
RNA-dependent RNA polymerase (syn. Quelling defective1)	*Fg*RdRP1	38%	FGSG_06504	Maybe associated with secondary sRNA production (Chen et al., 2015).
	*Fg*RdRP4	33%	FGSG_04619	Maybe associated with secondary sRNA production [40].
RNA dependent RNA polymerase (syn. Suppressor of ascus dominance, SAD1)	*Fg*RdRp2	42%	FGSG_08716	Maybe associated with secondary sRNA production (Chen et al., 2015).
	*Fg*RdRp5	29 %	FGSG_09076	Roles in the antiviral defence [65]. Maybe associated with secondary sRNA production (Chen et al., 2015).
RNA-dependent RNA polymerase (RRP3)	*Fg*RdRP3	47%	FGSG_01582	Maybe associated with secondary sRNA production (Chen et al., 2015).

bioRxiv preprint doi: https://doi.org/10.1101/633099; this version posted May 14, 2019. The copyright holder for this preprint (which was not certified by peer review) is the author/funder. All rights reserved. No reuse allowed without permission.

QDE2-interacting protein	*Fg*QIP	32%	FGSG_06722	The homolog has been identified in (Chen et al., 2015), but not yet studied in depth.
RecQ helicase QDE3	*Fg*QDE3	46%	FGSG_00551	not studied

777

bioRxiv preprint doi: https://doi.org/10.1101/633099; this version posted May 14, 2019. The copyright holder for this preprint (which was not certified by peer review) is the author/funder. All rights reserved. No reuse allowed without permission.

778 **Table 2:** Trichothecenes produced by RNAi mutants in infected wheat kernels at 13 dpi.
779

Samples	ng *Fg* DNA /mg seed d.w.	DON [mg/kg seed]	DON/DNA	[1]A-DON [mg/kg seed]	[2]A-DON/DON x1000
Mock (without *Fg*)	0	0.00	0	0	0
Δ ago1	0.84	12.7	15.2	0.45	36
Δ ago2	1.28	32.3	25.2	1.04	32
Δ dcl1	2.86	61.9	21.6	1.87	30
Δ dcl2	2.03	56.6	27.9	1.89	33
Δ rdrp1	4.84	86.7	17.9	3.51	40
Δ rdrp2	0.95	16.9	17.8	0.43	25
Δ rdrp3	0.78	12.3	15.6	0.35	29
Δ rdrp4	0.47	4.90	10.3	0.15	31
Δ qip	2.53	68.7	27.2	2.87	42
Δ qde3	4.33	82.3	19.0	3.91	47
IFA wt	2.18	78.3	35.9	2.58	33

780
781 DON, deoxynivalenol; A-DON, acetyldeoxynivalenol
782 [1] 3A-DON (3-acetyldeoxynivalenol) and 15A-DON (15-acetyldeoxynivalenol) were measured
783 [2] Ratio of concentrations of A-DON and DON, multiplied by 1000
784
785

bioRxiv preprint doi: https://doi.org/10.1101/633099; this version posted May 14, 2019. The copyright holder for this preprint (which was not certified by peer review) is the author/funder. All rights reserved. No reuse allowed without permission.

Supplement data:

Supplement figures

Figure S1:
Schematic representation of the gene replacement strategy used for *Fusarium graminearum* transformation. Yellow box: the target gene that has to be replaced by KO; dark green box: selection marker gene, in this case the antibiotic resistance gene (*hygromycin B phosphotransferase* of *E. coli*, hph). Blue arrow: Homologous recombination sequences, typically ~1 kb long; Black arrows: template area for primers binding used for transformants genotyping. PgpdA: Promoter region of the *Glyceraldehyde-3-phosphate dehydrogenase* gene of *Aspergillus nidulans*; TtrpC: termination region of the *Aspergillus nidulans trpC* gene.

Fig. S2. Compromised expression of deleted RNAi genes in *Fusarium graminearum* knockout (KO) mutants. Expression of the targeted genes in respective Fusarium mutants. Transcript levels were analyzed by qRT-PCR from five-day-old PEG liquid cultures and transcript quantified by normalization to Fusarium *β-Tubulin* (*FgTub*) or *Elongation factor a* (*FgEF1a*) and comparison to wt IFA65

Figure S3. Colony morphology and growth of RNAi knock-out (KO) mutants. Fusarium mutants and the wt IFA65 were grown for 5 days on solid (A) PDA (potato dextrose agar), (B) SN (synthetic nutrient), (C) CM (Aspergillus complete medium) and in liquid PEG medium without hygromycin. The mutants showed differences in pigmentation as follows: *Δago1*, *Δrdrp2*, *Δrdrp3* and *Δrdrp4* darker pigmentation; *Δdcl1*, *Δdcl2* and *Δrdrp1* reduced pigmentation compared to wt.

Fig. S4. Infection of wheat spikes with *Fusarium graminearum* RNAi mutants and wt strain IFA65. Thousand grain weight (TGW) of infected wheat spikes. Mock control: Kernels treated with 0.002% Tween 20; mature kernels: completely mature Apogee kernels.

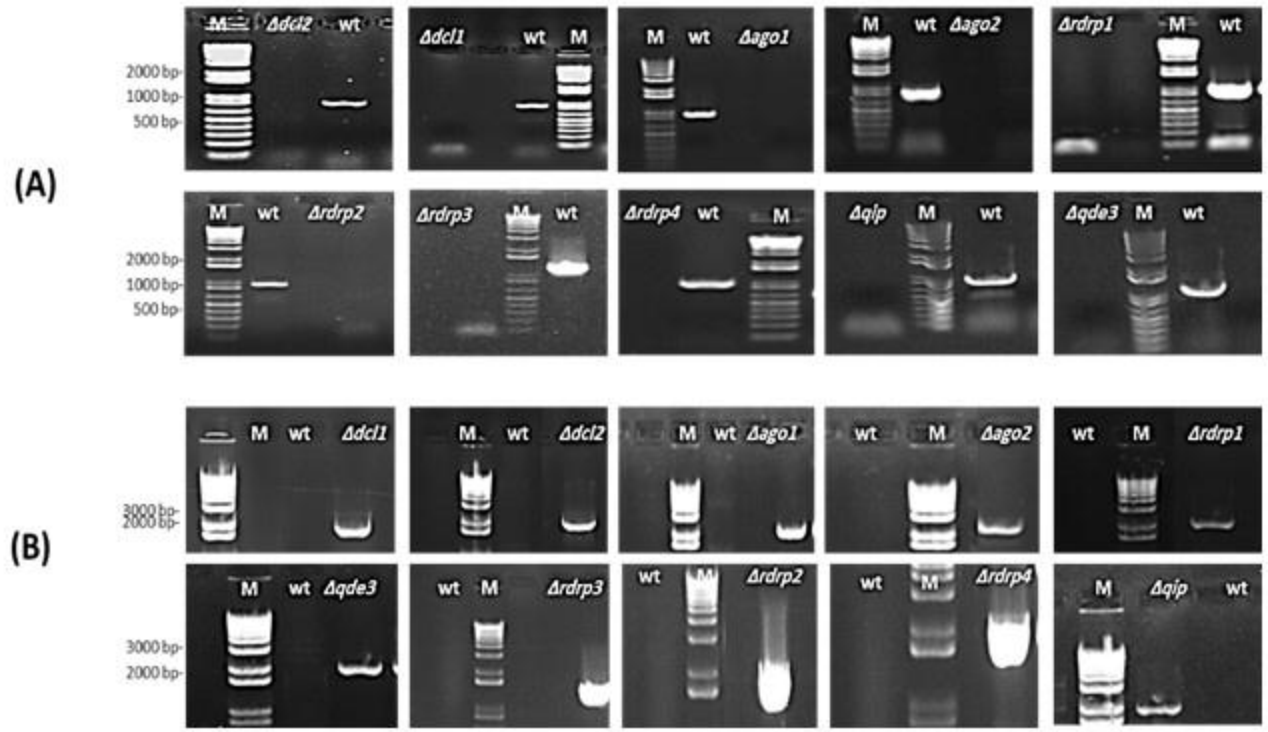
(A)
M Δdcl2 wt
Δdcl1 wt M
M wt Δago1
M wt Δago2
Δrdrp1 M wt
2000 bp
1000 bp
500 bp
M wt Δrdrp2
Δrdrp3 M wt
Δrdrp4 wt M
Δqip M wt
Δqde3 M wt
2000 bp
1000 bp
500 bp
(B)
M wt Δdcl1
M wt Δdcl2
M wt Δago1
wt M Δago2
wt M Δrdrp1
3000 bp
2000 bp
M wt Δqde3
wt M Δrdrp3
wt M Δrdrp2
wt M Δrdrp4
M Δqip wt
3000 bp
2000 bp

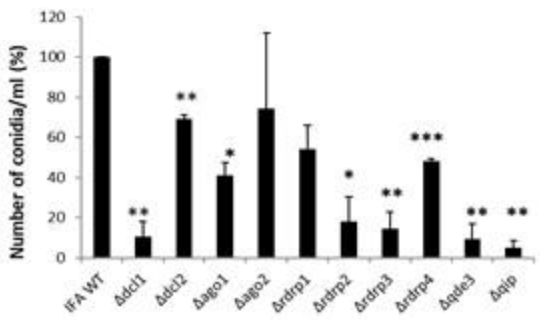

(A)

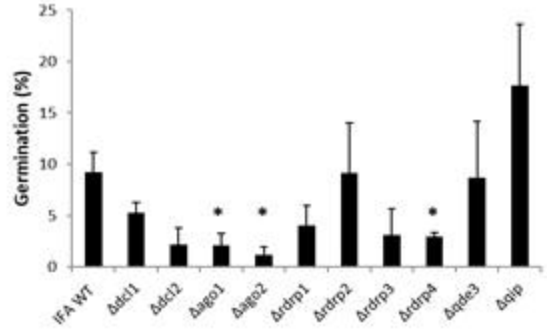

(B)

(C)

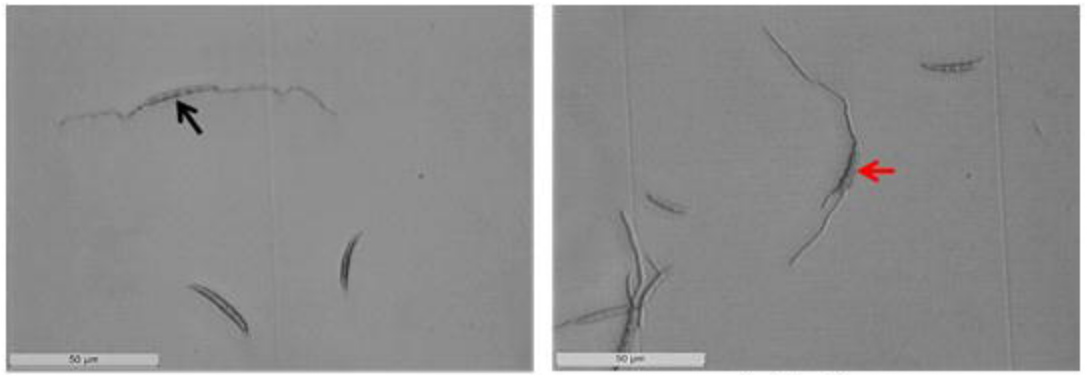

IFA wt

Δrdrp4

Fig. 2

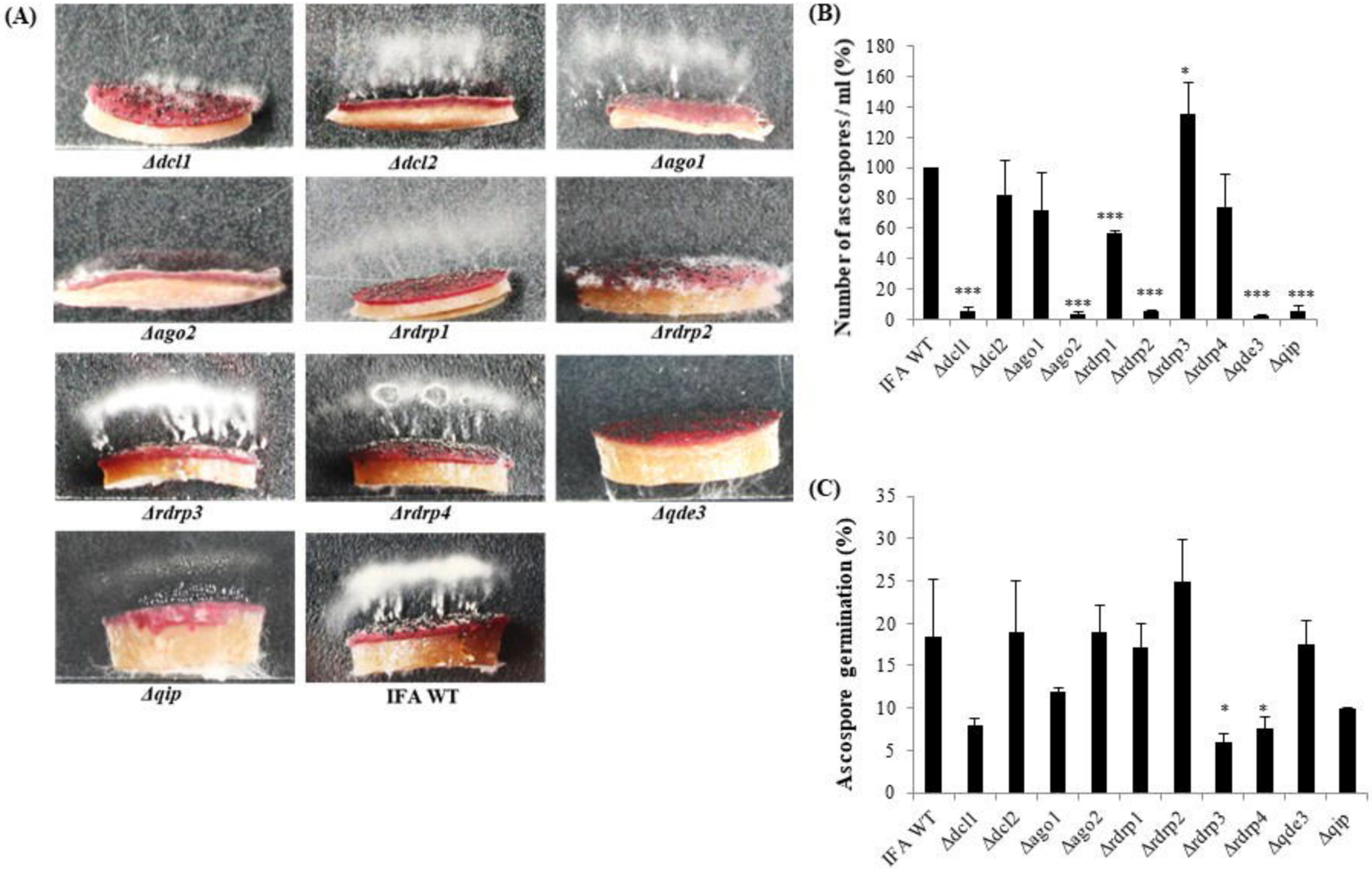
(A)
Δdcl1
Δdcl2
Δago1
Δago2
Δrdrp1
Δrdrp2
Δrdrp3
Δrdrp4
Δqde3
Δqip
IFA WT
(B)
Number of ascospores / ml (%)
180
160
140
120
100
80
60
40
20
0
***
*
IFA WT
Δdcl1
Δdcl2
Δago1
Δago2
Δrdrp1
Δrdrp2
Δrdrp3
Δrdrp4
Δqde3
Δqip
(C)
Ascospore germination (%)
35
30
25
20
15
10
5
0
*
IFA WT
Δdcl1
Δdcl2
Δago1
Δago2
Δrdrp1
Δrdrp2
Δrdrp3
Δrdrp4
Δqde3
Δqip

Fig. 3

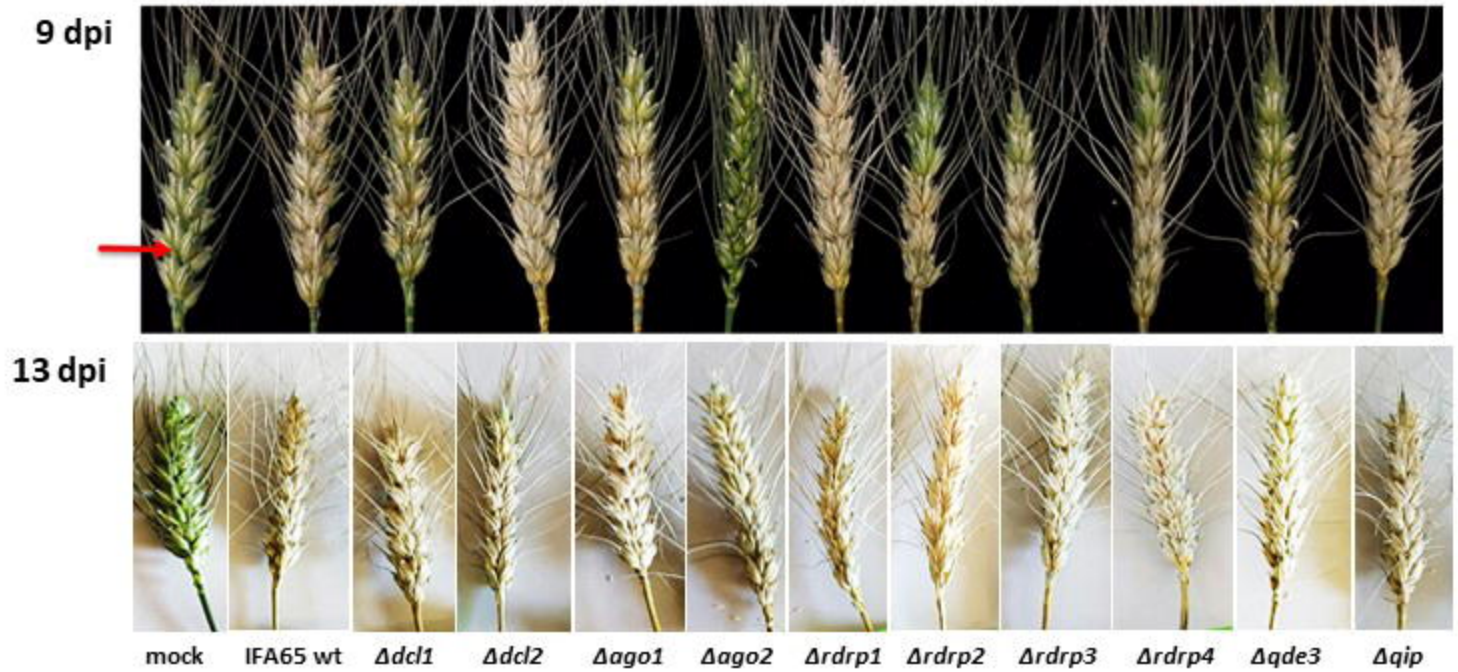
9 dpi
13 dpi
mock
IFA65 wt
Δdcl1
Δdcl2
Δago1
Δago2
Δrdrp1
Δrdrp2
Δrdrp3
Δrdrp4
Δqde3
Δqip

Fig. 4

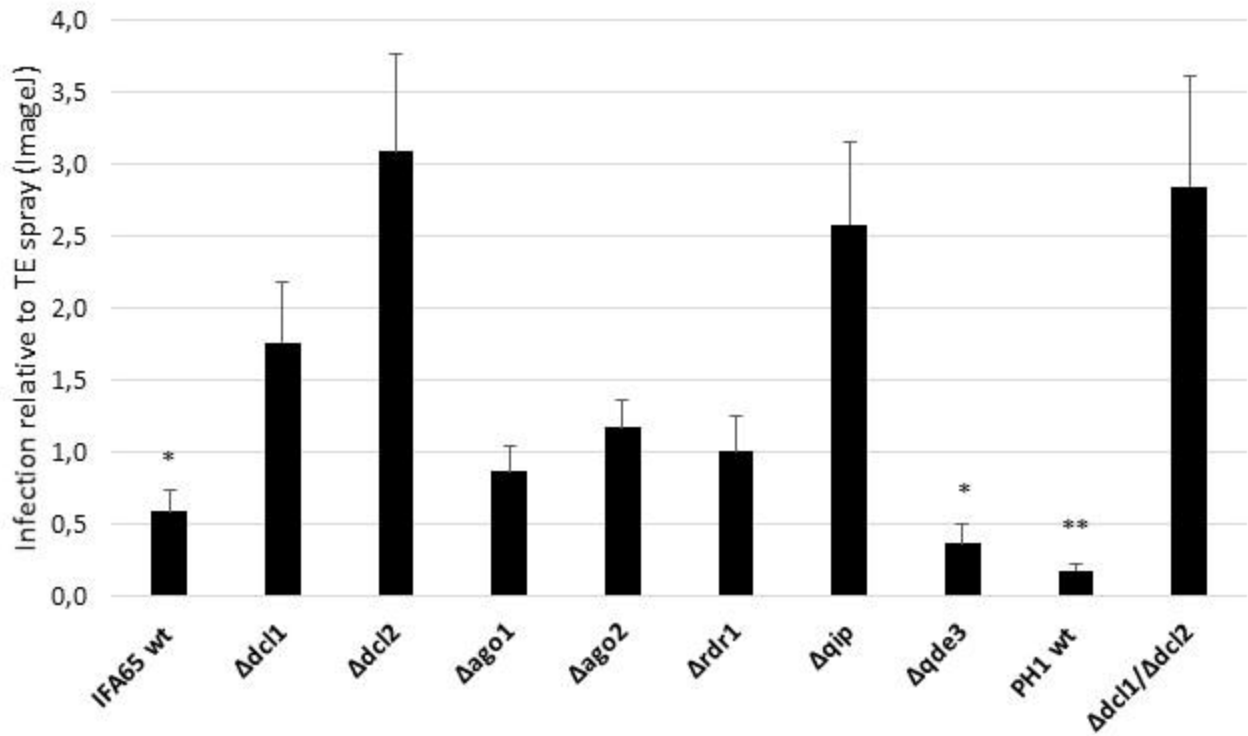
Infection relative to TE spray (ImageJ)
4,0
3,5
3,0
2,5
2,0
1,5
1,0
0,5
0,0
*
*
**
IFA65 wt
Δdcl1
Δdcl2
Δago1
Δago2
Δrdr1
Δqip
Δqde3
PH1 wt
Δdcl1/Δdcl2

Fig. 5A

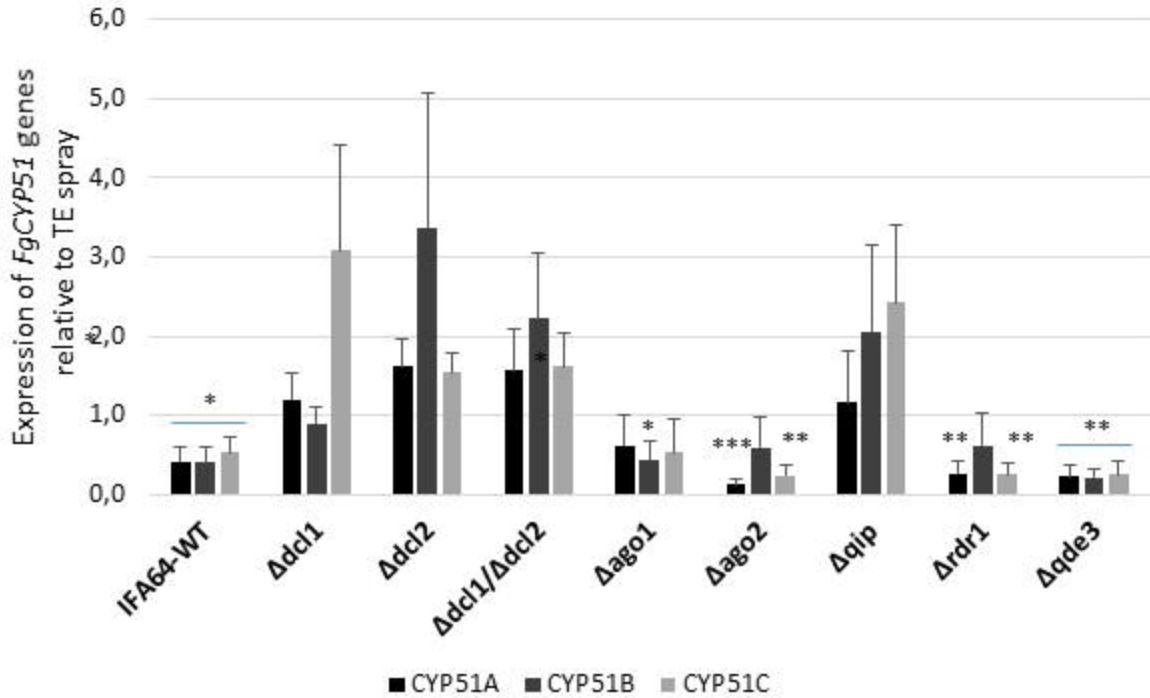
Expression of FgCYP51 genes relative to TE spray
6,0
5,0
4,0
3,0
2,0
1,0
0,0
IFA64-WT
Δdcl1
Δdcl2
Δdcl1/Δdcl2
Δago1
Δago2
Δqip
Δrdr1
Δqde3
CYP51A
CYP51B
CYP51C

Fig. 5B